Science of the Total Environment 670 (2019) 826–836

Contents lists available at ScienceDirect

Science of the Total Environment

journal homepage: www.elsevier.com/locate/scitotenv

Upland Soil Cluster Gamma dominates methanotrophic communities in upland grassland soils

Yongcui Deng [a,1], Rongxiao Che [b,c,d,1], Fang Wang [c,d], Ralf Conrad [e], Marc Dumont [f], Juanli Yun [g], Yibo Wu [h], Ang Hu [i], Jie Fang [a], Zhihong Xu [d], Xiaoyong Cui [c,j,k,*], Yanfen Wang [c]

[a] School of Geography, Nanjing Normal University, 210023 Nanjing, China
[b] Institute of International Rivers and Eco-security, Yunnan University, 650091 Kunming, China
[c] University of the Chinese Academy of Sciences, 100049 Beijing, China
[d] Environmental Futures Research Institute, School of Environment and Science, Griffith University, Brisbane 4111, Australia
[e] Max Planck Institute for Terrestrial Microbiology, Karl-von-Frisch Straße 10, 35043 Marburg, Germany
[f] Biological Sciences, University of Southampton, Southampton SO17 1BJ, United Kingdom
[g] Institute of Microbiology, Chinese Academy of Sciences, 100101 Beijing, China
[h] Ningbo University, 315211 Ningbo, China
[i] Hunan Agricultural University, 410128 Changsha, China
[j] CAS Center for Excellence in Tibetan Plateau Earth Sciences, Chinese Academy of Sciences, 100101 Beijing, China
[k] Research Center for Eco-Environmental Sciences, Chinese Academy of Sciences, 100085 Beijing, China

HIGHLIGHTS

- Aerobic methanotrophs in 30 grassland soils on the Tibetan Plateau were analyzed.
- USCγ dominated the methanotroph communities in the Tibetan grassland soils.
- USCγ also dominated in upland grassland soils around the world.
- Grassland methanotrophic communities are shaped by precipitation and soil pH.

GRAPHICAL ABSTRACT

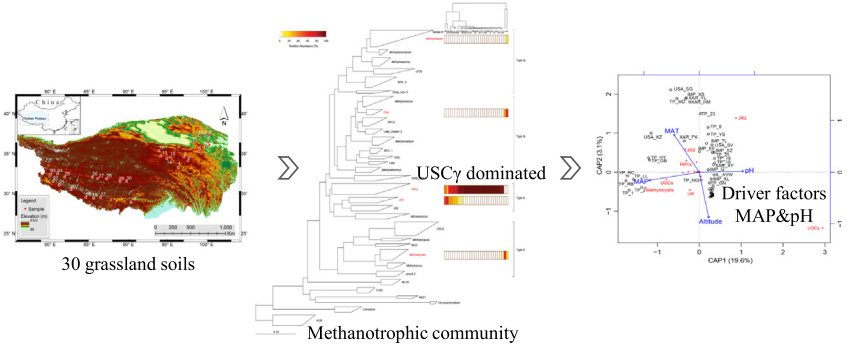

ARTICLE INFO

Article history:
Received 9 December 2018
Received in revised form 19 March 2019
Accepted 19 March 2019
Available online 20 March 2019

Editor: Ewa Korzeniewska

Keywords:
Methanotrophs
USCγ
Upland grassland soil

ABSTRACT

Aerobic methanotrophs in upland soils consume atmospheric methane, serving as a critical counterbalance to global warming; however, the biogeographic distribution patterns of their abundance and community composition are poorly understood, especial at a large scale. In this study, soils were sampled from 30 grasslands across >2000 km on the Qinghai-Tibetan Plateau to determine the distribution patterns of methanotrophs and their driving factors at a regional scale. Methanotroph abundance and community composition were analyzed using quantitative PCR and Illumina Miseq sequencing of *pmoA* genes, respectively. The *pmoA* gene copies ranged from 8.2×10^5 to 1.1×10^8 per gram dry soil. Among the 30 grassland soil samples, Upland Soil Cluster Gamma (USCγ) dominated the methanotroph communities in 26 samples. Jasper Ridge Cluster (JR3) was the most dominant methanotrophic cluster in two samples; while *Methylocystis*, cluster FWs, and *Methylobacter* were abundant in other two wet soil samples. Interestingly, reanalyzing the *pmoA* genes sequencing data from existing publications suggested that USCγ was also the main methanotrophic cluster in grassland soils in other

* Corresponding author at: University of the Chinese Academy of Sciences, 100049 Beijing, China.
E-mail address: cuixy@ucas.edu.cn (X. Cui).
[1] Rongxiao Che and Yongcui Deng contributed equally to this work.

https://doi.org/10.1016/j.scitotenv.2019.03.299

Qinghai-Tibetan Plateau
Biogeography

regions, especially when their mean annual precipitation was <500 mm. Canonical Analysis of Principal Coordinates including all soil samples indicated that the methanotrophic community composition was significantly correlated with local environmental factors, among which mean annual precipitation and pH showed the strongest correlations. Variance partitioning analysis showed that environmental factors and spatial distance were significant factors affecting the community structure of methanotrophs, and environmental properties were more important factors. Collectively, these findings indicate that atmospheric methane may be mainly oxidized by USCγ in upland soils. They also highlight the key role of water availability and pH in determining the abundance and community profiles of grassland soil methanotrophs.

1. Introduction

With an annual global budget of 500–600 Tg, methane (CH_4) is the second most prevalent greenhouse gas after carbon dioxide (Conrad, 2009; IPCC, 2014). In upland soils, its consumption by methane-oxidizing bacteria (methanotrophs) reaches ~30 Tg yr^{-1}, being the second largest sink of atmospheric methane after hydroxyl radical depletion (Wuebbles and Hayhoe, 2002). Methanotroph abundance and community composition have been recognized as key factors determining methane oxidation capacity in soils, and thus thorough understanding of them can substantially deepen our insights into the methane oxidation mechanisms.

As observed in multiple investigations, in upland soils, atmospheric methane was mainly oxidized by a set of methanotrophs that are currently uncultivated (Knief et al., 2003). These methanotrophs are mainly characterized by *pmoA* genes, encoding a ~26-kDa subunit of particulate methane monooxygenase (pMMO). According to the phylogenetic analyses of *pmoA* genes, these uncultivated methanotrophs have been classified into Upland Soil Clusters (USCα and USCγ) and Jasper Ridge Clusters (JR1, JR2 and JR3) (Horz et al., 2005; Knief et al., 2003; Holmes et al., 1999; Henckel et al., 2000). Their high affinity to methane and the potential to oxidize atmospheric methane have been proposed and verified (Dunfield, 2007; Kolb, 2009). Besides the uncultured methanotroph clusters, some *Methylocystis* species are also able to oxidize atmospheric methane by virtue of an additional divergent pMMO2 enzyme (Yimga et al., 2003; Baani and Liesack, 2008). Nevertheless, with most of the existing efforts being made to reveal the abundance and community compositions of methanotrophs in wetland soils, methanotrophs in upland soils remain far from well investigated.

The methanotroph communities in different ecosystems are influenced by environmental factors, including methane concentrations, metal ions, nutrient availability, pH, temperature, salinity, and water availability (Conrad, 2007; Knief, 2015; Semrau et al., 2010). Habitat preferences do exist for methanotrophic taxa (Knief, 2015). Considering hydromorphic soils, arctic-alpine soils, volcanic soils, and polluted soils as upland soils, different OTUs of USCα and USCγ are defined as habitat-specific in upland soils (Knief, 2015). Alpine grassland soil is also a typical upland soil. However, the abundance and community compositions of methanotrophs in upland grassland soils have rarely been systematically studied, let alone at regional scales. The Qinghai-Tibetan Plateau is the highest (~4000 m on average) and one of the largest plateaus (~2.6 × 10^6 km^2) in the world. >60% of its surface area is covered by alpine grasslands, most of which are classified as alpine steppe and alpine meadow ecosystems (Editorial Board of Vegetation Map of China, Chinese Academy of Sciences (EBVMC), 2001). Previous studies showed methane uptake rates of 71.5 ± 2.5 μg CH_4 m^{-2} h^{-1} in the alpine steppe soils and ~59.2 ± 3.7 μg CH_4 m^{-2} h^{-1} in the alpine meadow soils on the Qinghai-Tibetan Plateau (Wei et al., 2015). Although Tibetan methanotrophs have been investigated in a couple of alpine meadow soils (Kou et al., 2017; Zheng et al., 2012), their spatial distribution patterns and the factors that influence the methanotrophic distribution pattern have not been systematically examined. This seriously hampers our understanding of the methane uptake mechanism across the Qinghai-Tibetan Plateau.

This study aimed to reveal the geographical distribution pattern of methanotroph abundance and community composition, as well as the driving factors in grassland soils on the Qinghai-Tibetan Plateau. Soil samples were collected from 30 different sites (8 alpine meadows, 19 alpine steppes, and 3 desert steppes; Fig. 1) across the Qinghai-Tibetan Plateau. We applied quantitative PCR (qPCR) and Illumina Miseq sequencing of *pmoA* genes to determine the abundance and composition of the methanotroph communities in these samples, respectively. Additionally, the published *pmoA* sequencing data of methanotroph community composition in grassland soils on the Qinghai-Tibetan Plateau and other regions of the world were summarized, reanalyzed, and compared with the results in this study. Based on the aforementioned findings, the upland soil clusters of methanotrophs are habitat-specific and uniquely occur in soils exposed to low methane concentrations. We hypothesized that the methanotroph communities in grassland soils were dominated by different upland soil clusters of methanotrophs (i.e., USCα and USCγ).

2. Materials and methods

2.1. Sample collection and soil characterization

In total, 30 surface layer (0–5 cm) soil samples (8 alpine meadows, 19 alpine steppes, and 3 desert steppes) were collected on the Qinghai-Tibetan Plateau in August 2014 (Fig. 1, Table 1). The soil samples were randomly selected along the highway with 60–100 km intervals and a vertical distance of >500 m from the highway, as detailed in our recent publication (Che et al., 2018). The soils used for molecular analysis were kept at −20 °C during transportation and stored in the laboratory at −80 °C before DNA extraction. All the sampling sites were located by a GPS system recording the longitude, latitude, and altitude. Mean annual precipitation (MAP) and temperature (MAT) were obtained from China Meteorological Data Sharing Service System (http://data.cma.cn/site/index.html). Soil pH was determined at a soil to water ratio of 1:5 (W/V) using a pH monitor. Soil water content (SWC) was measured gravimetrically using ~10 g soil via oven-drying at 105 °C overnight. Soils used for carbon, nitrogen, and phosphorus analyses were air-dried and sieved through a 2-mm sieve to remove fine roots. Soil available phosphorus (AP) was measured as described previously (Olsen, 1954). Dissolved organic carbon (DOC) and dissolved total nitrogen (DTN) contents were analyzed using a TOC Analyzer (Liqui TOC II; Elementar Analysensysteme GmbH, Hanau, Germany). Ammonium (NH_4^+-N) and nitrate (NO_3^--N) were extracted from fresh soils and their contents were determined by a continuous flow analyzer. The number of plant species (NPS) was counted during sampling and the aboveground plant biomass (APB) was harvested and measured after oven-drying at 65 °C for 72 h in the laboratory.

2.2. DNA extraction and quantitative PCR

Total DNA was extracted from 0.3 g fresh soil using the PowerSoil™ DNA Isolation Kit (MO BIO Laboratories, Carlsbad, CA, USA). The copy numbers of *pmoA* gene were determined by real-time PCR with primer set A189f-mb661r and a SYBR Green System (Takara Bio Inc., Shiga,

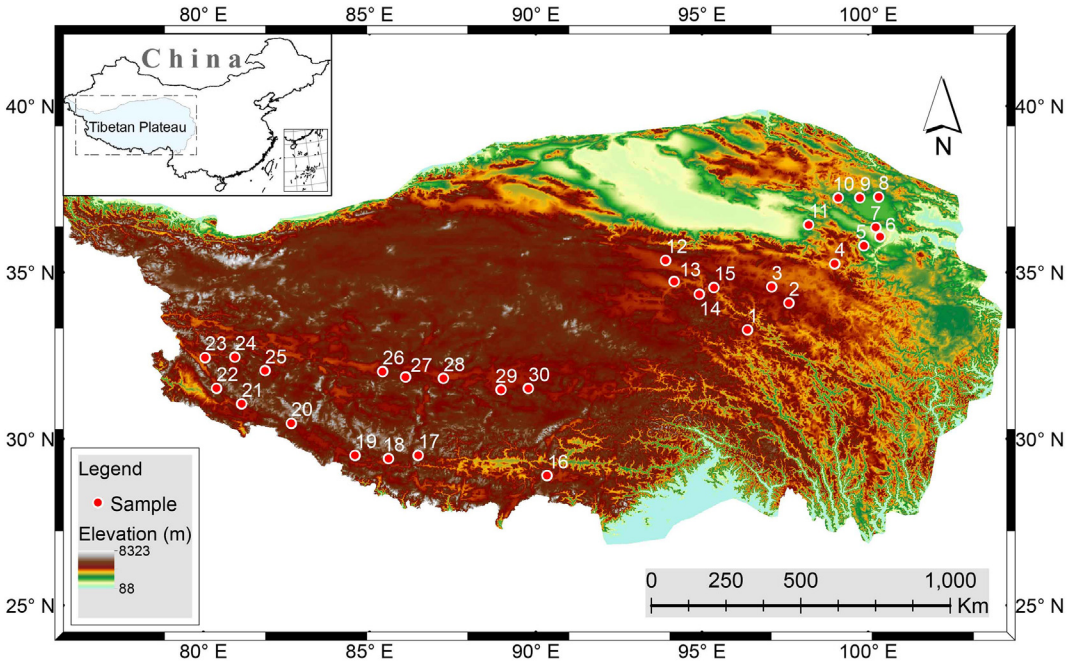

Fig. 1. The locations of 30 soil samples on the Qinghai-Tibetan Plateau.

Japan) as described previously (Kolb et al., 2003; Costello and Lidstrom, 1999). The assays were performed using a 7500 Real-Time PCR System (Applied Biosystems, Foster City, CA, USA) and the associated software. The 20-μl reaction mixtures contained: 1 μl template DNA, 10 μl SYBR Green and ROX mixture (2 ×, Takara Bio Inc., Shiga, Japan), 0.5 μl forward primer (20 μmol l^{-1}), 0.5 μl reverse primer (20 μmol l^{-1}), and 8 μl nuclease-free water. Standard curves were constructed using plasmids harboring the *pmoA* gene fragment. PCR runs started with an initial denaturation and enzyme activation step at 95 °C for 30 s, followed by 40 cycles of 5 s at 95 °C, 30 s at 54 °C, 40 s at 72 °C, and 30 s at 80 °C. We recorded the fluorescence signal at 80 °C to attenuate influences of primer dimers. The specificities of PCR products were tested by melting curve analysis. The R^2 and amplification efficiency of the standard curve were 0.99 and 96.2%, respectively.

2.3. Illumina sequencing and bioinformatic analyses

Primer pairs A189f-mb661r were designed for the detection of type I and type II methanotrophs and were also used for Illumina sequencing analysis. The *pmoA* gene fragment from each soil sample was amplified using an A189f primer with individual barcode for identification. PCRs were performed in 50 μl reaction volumes containing 25 μl Premix Taq™ Hot Start Version (Takara Bio Inc., Shiga, Japan), 1 μl each primer (20 μmol l^{-1}), and 1 μl of template. Cycling was performed with an initial denaturation at 95 °C for 10 min followed by 38 cycles: 94 °C 30 s, 52 °C 30 s, 72 °C 45 s, and a final extension at 72 °C for 10 min on a Bio-Rad C1000 instrument; however, A189f-mb661r primer set is specific for *pmoA* but discriminates against USCα methanotrophs (Costello and Lidstrom, 1999; Bourne et al., 2001). In contrast, the primer set A189-A682r offers a broader coverage which covers USCα methanotrophs (Holmes et al., 1995); however, primer pair A189f-A682r also target *amoA* genes of ammonia-oxidizing bacteria. The primer 650r was designed to target USCα methanotrophs (Bourne et al., 2001). In order to target a broad range of *pmoA* sequences including USCα methanotrophs, but fewer *amoA* sequences, we also amplified *pmoA* genes via a seminested PCR approach using primer pair A189-A682r for the 1st round PCR and A189f-mb661r/650r primer systems as the 2nd round. This combination allowed simultaneous amplification of a broad range of *pmoA* targets. The first round was performed using same PCR protocol as described above for primers pair A189f-mb661r. PCR products were then purified using the GeneJET Gel Extraction Kit (Thermo Scientific, Lithuania). Aliquots of the first round of PCR (2 μl) were used as the template for the second round of PCR with forward primer A189f and the two reverse primers mb661r and 650r in a multiplex PCR setting. The second-round PCRs were performed in 50-μl volumes containing 25 μl Premix Taq™ Hot Start Version (Takara Bio Inc., Shiga, Japan), 1 μl of forward primer A189f with barcode (20 μmol l^{-1}), 0.5 μl of primer mb661r, 0.5 μl of primer 650r, and 2 μl of purified PCR product of the first-round PCR. Cycling of the second-round PCR was performed at 95 °C for 10 min followed by 20 cycles: 94 °C 30 s, 52 °C 30 s, 72 °C 45 s, and a final extension at 72 °C for 10 min. Three technical replicates were conducted for each sample, and the technical replicates were then separately pooled into one tube. Subsequently, PCR products obtained from two primer sets were all purified using the GeneJET Gel Extraction Kit (Thermo Scientific, Lithuania). Finally, samples were pooled in equimolar concentrations for paired-end sequencing (2 × 300 bp) on the Illumina MiSeq platform at the Chengdu Institute of Biology, Chinese Academy of Sciences.

Sequence processing was based on recommendations of the UPARSE OTU analysis pipeline (Edgar, 2013) and additionally included tools from the programs of Mothur (v. 1.27) (Schloss et al., 2009), USEARCH v8.0.1623 (Edgar, 2010), and ARB-5.5 (Ludwig et al., 2004). Paired-end reads were first merged using USEARCH -fastq_mergepairs command with default setting. Sequences were then sorted based on barcodes and forward primer. All sequences with a maximum expected error >1 or length shorter than 471 bp were removed by using the -fastq_filter option. Dereplication with removal of singletons was carried out by -derep_fulllength and the -sizeout option. First, *pmoA* gene operational taxonomic units (OTU) representatives were obtained by using -cluster_otus at 98% sequence identity with inherent de novo chimera detection in USEARCH. A further chimera check was performed by -uchime_ref command using ~4000 *pmoA* and related sequences as the reference database. These 98% level *pmoA* OTU representatives were then imported into ARB and translated to amino acid sequences to further check the sequences mistakes and chimeras. Only the high-quality OTU representatives were used to calculate distances matrices in ARB based on the 157 amino acid residues. New OTUs were assigned at 0.18 amino acid distance levels using the average linkage algorithm

implemented in Mothur. Neighbor-joining phylogenetic trees based on new represented OTU-sequences in our soil samples and related sequences were built in ARB (Ludwig et al., 2004). The relative abundances of new OTUs were determined by mapping all *pmoA* gene sequences to the OTU representatives using -usearch_global with the gene 0.82 OTU thresholds. The classification of sequencing reads was double checked using the Bayesian/Wang methods (cutoff = 80%), based on a taxonomy database including >4000 *pmoA* and related sequences (Deng et al., 2013; Lüke and Frenzel, 2011). The sequences obtained from the two step PCRs (1st step with primers A189f-a682r and 2nd step with primers A189f-mb661r/650r) were also classified based on this *pmoA* taxonomy database. The Illumina sequencing reads (raw data) were deposited under the study number SRP098625 in the NCBI Sequence Read Archive.

2.4. Published pmoA data collection and analysis

Besides *pmoA* data that were obtained in this study, the *pmoA* sequence data published in other grassland soils were collected from the literature. First, we conducted a literature search in Web of Science databases using the query expression "(grassland* OR steppe* OR meadow* OR prairie* OR rangeland*) AND (methanotroph* OR methane-oxidizing bacteria OR *pmoA*)" (June 3, 2018). Only *pmoA* sequencing data based on the primer sets A189f-mb661r, A189f-A682r or a combination of both primers were included. Only those studies based on DNA extracted from in-situ soils were included, while those based on DNA extracted from enrichments of soils or based on RNA were not included. In total, 33 soil samples were added to the analysis, in which twenty-seven samples are from grasslands in China, including 11 samples from Tibetan Plateau (TP_, Kou et al., 2017; Zheng et al., 2012), 5 from Xinjiang Autonomous Region (XAR_, Kou et al., 2017), 9 from Inner Mongolia Plateau (IMP_, Kou et al., 2017; Ma et al., 2016) and 2 from Yunnan Plateau (YN_RB and YN_RB, Dai et al., 2015). The other 6 samples were from Negev Desert Plateau in Israel (IL_AVW and IL_AVO, Angel and Conrad, 2009), Konza Prairie in Kansas, Shortgrass Steppe in Colorado and Sevilleta in New Mexico (USA_KZ, USA_SG, USA_SV, Judd et al., 2016) and upland tundra in Canada (CAN_UT, Martineau et al., 2014). All the location information of sampling sites was collected from the literature. The mean annual precipitation (MAP) and temperature (MAT) were taken from the literature or obtained from the Climate Research Unit (CRU TS 4.02, https://crudata.uea.ac.uk/cru/data/hrg/). The elevation information was obtained from the literature or the GTOPO30 dataset (https://lta.cr.usgs.gov/GTOPO30). The pH values of each sample were collected from the literature. The *pmoA* sequences from the published literature were all downloaded from the website of the National Center for Biotechnology Information (NCBI) according to the submitted Genbank number or SAR number listed in the literature. All these sequences were classified using the Bayesian/Wang methods (cutoff = 80%), based on the *pmoA* taxonomy database (Deng et al., 2013; Lüke and Frenzel, 2011).

2.5. Statistical analysis

The relationships between methanotroph abundance and environmental factors were analyzed by spearman correlation using the "agricolae" package of R. The relative importance of environmental variables shaping the methanotroph community was estimated using Canonical Analysis of Principal Coordinates (CAP, Anderson and Willis, 2003). The plot of CAP, also called Distance-based redundancy analysis (db-RDA), based on Bray-Curtis distance of methanotroph community profiles, was generated using the "capscale" function in Vegan package of R (Oksanen et al., 2014). Only four environmental factors including MAP, MAT, altitude and pH were available for all the soils, including our 30 collected samples and the additional 33 retrieved from the literature, so they were used to perform the CAP ordination plot for all the 63 soil samples. Meanwhile, for the 30 collected soil samples on the Qinghai-Tibetan Plateau, the effects of 13 environmental factors listed in the columns 4–16 of Table 1 were also tested. The methanotroph community data used in this part were transformed by the Hellinger distance before being used for analysis.

In order to test the significance of the correlation between the community dissimilarity and geographic or environmental distance, Mantel tests were conducted between community dissimilarity matrix and geographic distance matrix or environmental dissimilarity matrix (Legendre and Fortin, 2010). Community dissimilarity matrix was calculated based on the Bray Curtis distance (Bray and Curtis, 1957) of methanotroph community data. The Vincenty formula for distance between two latitude/longitude points was used to calculate the geographic distance matrix (Vincenty, 1975). The environmental dissimilarity matrix was calculated as the Euclidean distance (Deza and Deza, 2009) based on 4 environmental factors MAP, MAT, altitude and pH collected in all samples. All these environmental variables were standardized before the calculation. Fig. 5 showing these correlations was performed by "ggplot" function in ggplot2 package of R (Wickham, 2009).

Principal coordinates of neighbor matrices (PCNM) analyses were conducted based on principal coordinate analysis (PCoA) of the truncated geographic distance matrix. The PCNMs were then used as explanatory variables to variation partitioning. Variation partitioning (Legendre and Legendre, 2012) was performed in R with an environmental data set and two subsets of spatial variables. It quantified the unique or combined proportions of variation explained by the environmental factors, a linear trend and the PCNM spatial factors. The variables within each data set were independently forward selected based on the CAP model using the forward.sel command in the packfor package (Dray et al., 2011).

3. Results

3.1. Abundance of methanotrophs

The abundance of methanotrophs in 30 soil samples was represented by *pmoA* gene copies, which were determined using qPCR. The values were in the range of 8.2×10^5 to 1.1×10^8 copies per gram dry weight soil (Table 1). On average, the abundance of methanotrophs in the alpine steppe and meadow soils was higher (10^7 *pmoA* copies per gram dry soil) than in the alpine desert soils (10^6 *pmoA* copies per gram dry soil). Spearman correlation analysis indicated that the methanotroph abundance was significantly positively correlated with soil water content, total organic carbon, total nitrogen, dissolved total nitrogen, dissolved organic nitrogen and number of plant species ($p < 0.05$).

3.2. Soil methanotroph community composition

With the first primer set A189f-mb661r, in total of 937,140 sequences were obtained in 30 soil samples on the Qinghai-Tibetan Plateau. Among them, 916,906 sequences were classified into different *pmoA* clusters, with an average of 31,238 sequences per sample (Supplement 1). Based on 18% dissimilarity at the amino acid level, five OTUs were identified and added to the *pmoA* tree (Fig. 2). The most abundant *pmoA* cluster was USCγ, accounting on average to 90.4% of the methanotroph sequences in 28 upland grassland soils, while JR3 was only relatively abundant in a few soils (sample ID 6, 7, 18, 19, 23, 24, 25, 28, 29). Using Manhattan distance and Centroid cluster method, the methanotroph community composition of relatively wet grassland soils (sample ID 1, 2) were clustered separately from other soils (Fig. 2). In samples 1 and 2, the relative abundances of *Methylocystis*, cluster FWs, and *Methylobacter* were significantly higher than that in the other soils. This classification was confirmed with blast analysis against a large *pmoA* sequence database, and using the Bayesian/Wang method (cutoff = 80%; Supplement 1). Using the second primer set (1st A189f-a682r and then 2nd A189f-mb661r/650r), USCγ was also

Table 1
The environmental characteristics of 30 sampling soils on the Qinghai-Tibetan Plateau.

ID	Location	*pmoA* gene copies g^{-1} dry soil	Altitude (m)	Mean Annual Precipitation (mm)	Mean Annual Temperature (°C)	Soil Water Content (%)	Available Phosphorus (mg/kg)	Total Organic Carbon (g/kg)	Total Nitrogen (g/kg)	Dissolved Organic Carbon (mg/kg)	Dissolved Total Nitrogen (mg/kg)	NH_4^+-N (mg/kg)	NO_3^--N (mg/kg)	Dissolved Inorganic Nitrogen (mg/kg)	Dissolved Organic Nitrogen (mg/kg)	pH	Aboveground Plant Biomass (g/m^2)	Number of Plant Species	Vegetation Types
1	N33°16′, E96°21′	6.5×10^7	4225	529.0	−2.8	201.7	40.7	239.0	5.0	682.6	49.6	12.9	13.9	26.8	22.7	7.7	240.2	8	Alpine meadow
2	N34°04′, E97°36′	6.6×10^7	4668	520.7	−4.0	159.0	35.7	154.0	6.7	1751.7	156.8	41.4	2.0	43.4	113.5	7.7	97.8	7	Alpine meadow
3	N34°34′, E97°05′	4.4×10^6	4314	385.1	0.2	16.7	6.6	23.3	2.2	330.1	22.9	2.5	3.4	5.9	17.0	8.4	134.6	12	Alpine meadow
4	N35°15′, E98°59′	1.1×10^7	4270	470.5	−0.2	11.3	4.5	13.2	1.1	308.1	20.0	7.6	9.5	17.1	2.9	8.3	234.9	18	Alpine meadow
5	N35°48′, E99°51′	8.1×10^7	3631	325.3	−0.2	13.0	4.6	15.5	1.7	138.4	22.1	2.8	6.3	9.1	13.0	8.5	89.3	12	Alpine steppe
6	N36°04′, E100°21′	2.3×10^7	2992	353.3	−0.2	14.9	3.8	14.4	1.7	205.4	14.0	4.3	19.1	23.5	0.0	9.1	65.0	4	Alpine steppe
7	N36°21′, E100°13′	6.5×10^7	3179	382.1	−0.2	26.9	6.3	32.1	3.2	109.3	19.9	2.8	6.8	9.6	10.3	8.6	83.9	12	Alpine steppe
8	N37°16′, E100°18′	6.3×10^7	3240	339.6	−2.2	3.9	9.0	32.7	3.3	160.8	29.6	2.3	2.0	4.3	25.3	8.6	99.7	15	Alpine steppe
9	N37°14′, E99°44′	4.7×10^7	3218	413.5	−2.2	7.2	8.9	51.4	4.2	212.5	42.6	2.0	1.1	3.2	39.5	8.6	152.0	26	Alpine steppe
10	N37°14′, E99°05′	5.9×10^7	3394	339.6	−3.6	3.0	12.3	47.2	4.4	242.4	44.6	1.6	1.4	3.0	41.6	8.2	94.7	20	Alpine meadow
11	N36°26′, E98°12′	1.2×10^7	3203	327.4	1.9	0.4	4.9	5.7	0.5	190.4	15.2	5.8	1.3	7.1	8.1	8.8	74.1	14	Alpine steppe
12	N35°21′, E93°54′	1.3×10^7	4501	230.2	−2.3	12.5	2.5	5.8	0.6	69.9	12.6	2.3	5.6	7.9	4.7	8.9	121.7	8	Alpine steppe
13	N34°43′, E94°09′	1.6×10^7	4778	422.2	−3.6	23.1	6.5	21.5	1.8	135.5	16.2	13.4	8.0	21.4	0.0	8.6	424.1	15	Alpine steppe
14	N34°20′, E94°55′	1.1×10^7	4315	468.7	−3.7	19.6	7.4	20.5	2.2	140.0	17.8	14.8	16.4	31.2	0.0	8.4	105.5	12	Alpine meadow
15	N34°32′, E95°21′	1.7×10^7	4198	412.8	0.0	17.5	6.8	32.6	2.9	168.1	27.7	11.9	13.4	25.3	2.4	8.6	101.9	6	Alpine steppe
16	N28°53′, E90°20′	3.7×10^7	4629	357.9	−0.1	29.6	6.3	14.3	1.3	244.2	16.6	6.1	9.0	15.1	1.4	7.9	44.1	26	Alpine meadow

17	N29°30′, E86°27′	6.5×10^7	4402	271.0	−1.4	18.4	6.0	42.2	3.0	404.7	41.2	20.0	5.0	25.0	16.2	6.8	40.9	14	Alpine meadow
18	N29°24′, E85°33′	3.1×10^6	4830	257.6	−2.9	21.2	8.1	7.2	0.5	294.3	15.9	4.1	5.0	9.1	6.8	7.4	69.3	13	Alpine steppe
19	N29°30′, E84°33′	3.2×10^6	4603	260.6	−2.5	7.0	3.3	4.6	0.4	131.9	8.6	5.0	4.3	9.3	0.0	7.6	40.3	9	Alpine steppe
20	N30°27′, E82°38′	2.9×10^7	4831	188.5	−4.5	8.5	7.8	8.5	0.7	212.3	14.0	2.1	4.4	6.5	7.5	8.2	40.1	5	Alpine steppe
21	N31°03′, E81°08′	1.2×10^7	4778	119.6	−3.2	14.3	7.8	15.3	1.5	134.1	13.8	6.6	5.6	12.1	1.7	8.0	31.1	18	Alpine steppe
22	N31°31′, E80°23′	1.8×10^7	4597	119.7	−2.9	8.2	5.7	17.5	1.0	250.3	12.6	1.9	3.2	5.1	7.5	8.8	10.6	3	Alpine steppe
23	N32°26′, E80°02′	2.9×10^6	4567	116.2	−2.9	1.3	3.0	1.8	0.2	90.9	8.8	3.2	3.6	6.9	2.0	8.9	22.0	4	Alpine desert
24	N32°27′, E80°56′	8.2×10^5	4490	109.1	−3.0	4.0	3.6	3.1	0.3	114.3	4.4	2.1	3.2	5.3	0.0	9.2	3.2	2	Alpine desert
25	N32°03′, E81°51′	5.8×10^6	4639	118.7	−2.8	5.2	5.1	6.8	0.7	194.4	10.0	3.7	6.3	10.0	0.0	8.8	25.5	3	Alpine steppe
26	N32°01′, E85°23′	3.0×10^7	4824	223.0	−3.0	9.3	6.2	12.6	1.6	253.6	15.0	2.6	6.9	9.5	5.6	8.7	31.9	21	Alpine steppe
27	N31°51′, E86°04′	1.1×10^8	4686	237.6	−3.4	14.1	3.8	12.6	1.6	142.1	12.2	2.5	7.3	9.8	2.4	8.7	37.6	21	Alpine steppe
28	N31°49′, E87°13′	7.7×10^6	4549	278.9	−3.1	5.9	2.2	3.3	0.4	110.8	9.6	1.6	1.8	3.4	6.2	8.8	12.9	6	Alpine desert
29	N31°28′, E88°57′	4.4×10^7	4564	358.4	−0.6	10.1	3.5	6.7	0.7	204.9	10.9	2.4	3.5	5.9	5.0	8.6	34.1	29	Alpine steppe
30	N31°31′, E89°46′	8.6×10^7	4499	367.8	−3.0	20.9	3.6	18.6	2.1	321.1	21.5	4.6	12.8	17.4	4.1	8.6	16.5	18	Alpine steppe

detected as overwhelmingly dominant in 28 upland grassland soils, accounting on average to 94.6% of the methanotroph sequences (Supplement 1).

In addition to our data from 30 samples on the Qinghai-Tibetan Plateau, other published methanotroph *pmoA* sequencing data from 33 grassland soils were also collected and summarized with our data (Fig. 3). These data included two sequencing methods, namely Miseq and Sanger. Relatively few *pmoA* sequences (on average 33) were obtained by Sanger compared with Miseq sequencing (on average 4835, Supplement 1). The sample ID in Fig. 3 are arranged from left to right along MAP gradient from the highest MAP (1069 mm) to the lowest MAP (87 mm). Among the 63 samples there were 8 with MAP >500 mm (we named them high MAP samples). Their MAP was 720 ± 253 (Mean ± SD), significantly higher ($p = 0.002$) than the other 55 samples with MAP value of 307 ± 122 (Mean ± SD). The pH value of these was 6.3 ± 1.0 (Mean ± SD), which was lower ($p = 0.001$) than that of the other 55 samples (8.1 ± 0.8, Mean ± SD). Among them, only one sample (TP_GN) with MAP of 620 mm, had USCγ as the dominant methanotrophic cluster. *Methylocystis, Methylobacter, Methylococcus*, cluster FWs, or USCα dominated the 7 other samples. In total, there were 55 samples with MAP <500 mm (we named them low MAP samples). The relative abundance of USCγ was clearly dominant in low MAP samples compared with high MAP samples. In addition to USCγ, potential atmospheric methane-oxidizing JR3 was also relatively abundant in some low MAP samples. Among the 55 low MAP samples, there were 31 samples with the relative abundance of USCγ larger than 90%, and 47 samples with the sum of the relative abundance of USCγ and JR3 larger than 90%. Also, USCα and JR2 were dominant in the low MAP samples TP_GB and USA_SG, respectively.

3.3. The influence of environmental properties and spatial distance on soil methanotroph communities

For all the 63 soil samples summarized in this study, CAP was used to visualize the environmental effects on the methanotroph community composition (Fig. 4A). The soil methanotroph community composition was significantly influenced by environmental factors including MAP (independent explanation of the variation: 21.7%), pH (16.3%), MAT (8.0%), and altitude (4.8%). The total contribution of all these four environmental factors to the variation in the methanotroph community matrix was 31.7%, of which CAP1 accounted for 24.9% and CAP2 for 4.6%. The arrows of environmental factors in the CAP plot showed the correlations between the environmental variables and the community variation, indicating that the relative abundance of cluster USCγ was higher in soils with relatively low MAP and MAT, as well as high pH values. The relative abundance of cluster JR3 was higher in soils with relatively low MAP, as well as high MAT and pH values. In contrast, *Methylocystis* methanotrophs were more abundant in soils with relatively high MAP and low pH values. The CAP demonstrated a separation of the methanotroph community structures between the soil samples with relatively high MAP and low pH values (sample ID YP_RB and RC; TP_1, 2, LL) and the other soils (Fig. 4A). All these results suggest that MAP and pH values were the important environmental factors that shape the methanotroph community composition in the grassland soils. CAP analyses based only on our 30 soil samples collected on the Qinghai-Tibetan Plateau were also conducted. All the 16 environmental factors included in Table 1 explained 94.6% of the soil methanotroph community composition (Fig. 4B, $p = 0.001$). Among them, 11 environmental factors significantly influenced the soil methanotroph community composition ($p < 0.05$). Soil water content (SWC) was the most influencing factor and explained 63.7% of methanotroph community composition ($p = 0.004$). SWC and MAP were negatively correlated with the relative abundance of USCγ and JR3 methanotrophs. Meanwhile, the soil nutrient contents including carbon, nitrogen, and phosphorus were also negatively correlated with the relative abundance of USCγ and JR3 methanotrophs (Fig. 4B); however, altitude (Alti), mean

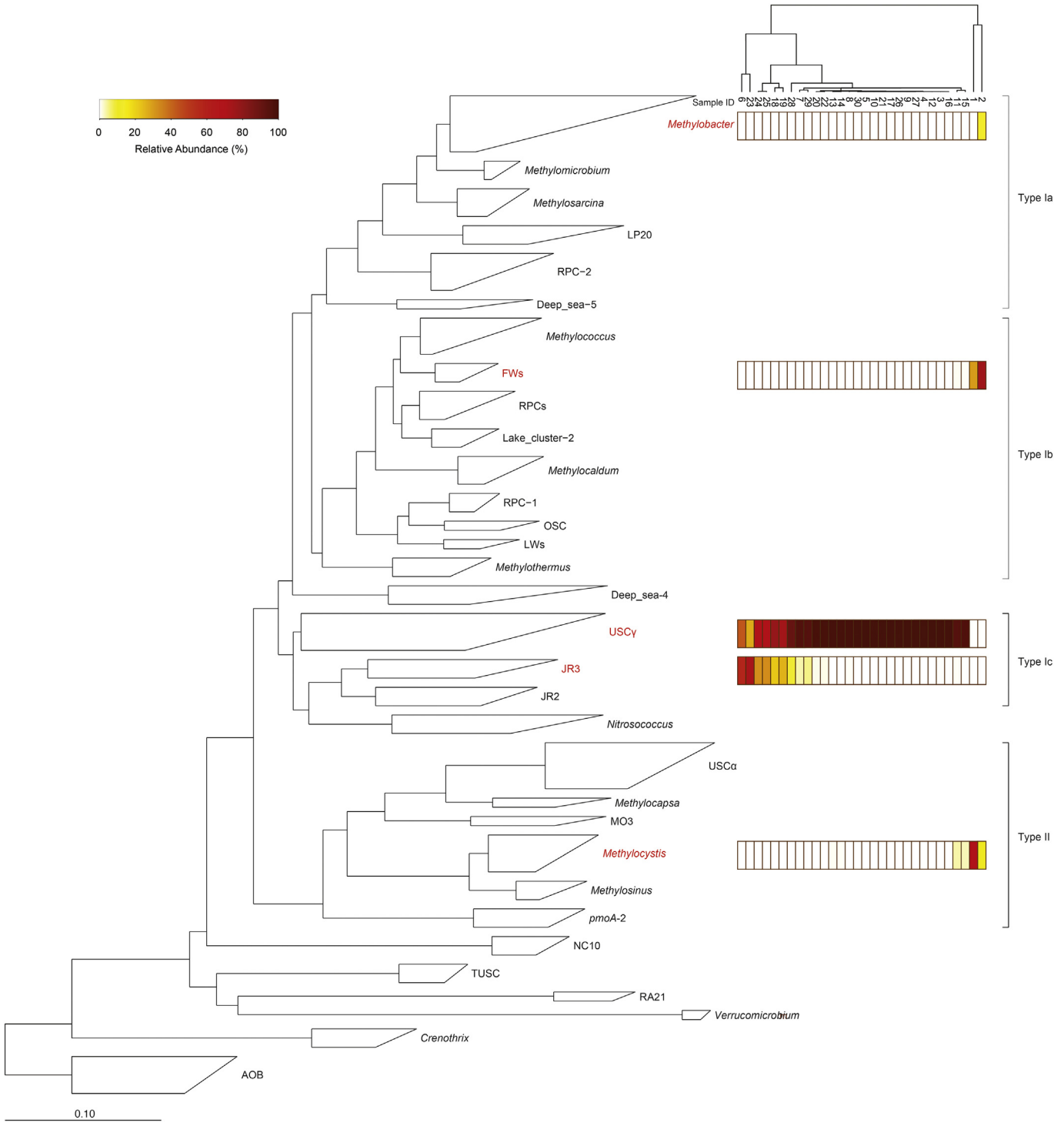

Fig. 2. *pmoA* gene neighbor-joining phylogenetic tree based on 157 deduced amino acid positions of five represented OTU-sequences and other ~2500 related sequences obtained from public databases. The phylogenetic tree construction was performed in ARB. The heatmap next to the phylogenetic clusters shows the relative abundance of the sequences assigned to each OTU based on Illumina sequencing analyses. The colour key from white to red indicates the relative abundance of each OTU from low to high, respectively. The five represented OTUs that were found in upland soils are marked in red and sample ID are listed on the top of the heatmap plot indicating the different soil samples from which the OTUs originated. The acronyms of different *pmoA* genes clusters were described previously (Lüke and Frenzel, 2011; Deng et al., 2013; Dumont et al., 2014). (For interpretation of the references to colour in this figure legend, the reader is referred to the web version of this article.)

annual temperature (MAT), nitrate (NO_3^--N), pH, and the aboveground plant biomass (APB) were not significantly correlated with the soil methanotroph community composition ($p > 0.05$).

The effects of geographic distance and environmental distance on the methanotroph community dissimilarity were compared (Fig. 5). The community dissimilarity increased with increasing geographic and environmental distance. The Mantel tests demonstrated that the methanotroph community composition showed stronger correlations with local environmental factors ($r = 0.37$, $p = 0.001$) than geographic distance ($r = 0.16$, $p = 0.046$).

Variance partitioning analysis based on the CAP model was conducted to assess the contribution of environmental properties and spatial distance to methanotroph community variation (Fig. 6). In a forward selection procedure, three environmental variables (MAP, pH,

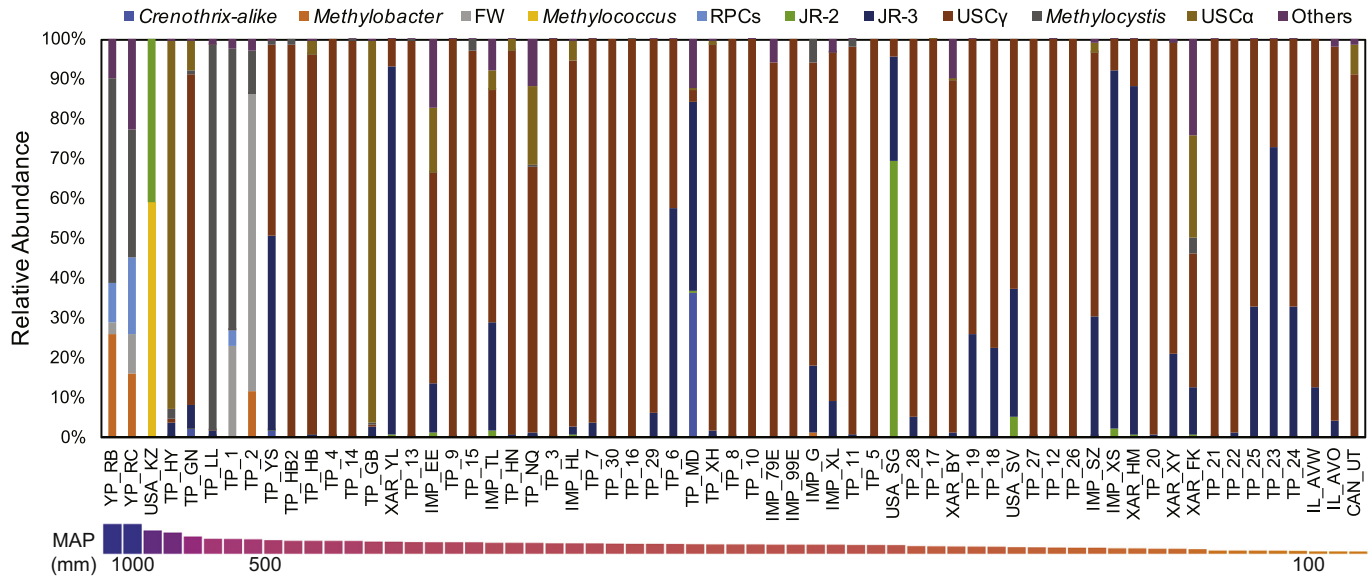

Fig. 3. The relative abundance of methanotrophic clusters in 63 grassland and desert soil samples. The classification of *pmoA* sequences used the Bayesian/Wang methods (cutoff = 80%) based on a taxonomy database including >4000 *pmoA* and related sequences (Deng et al., 2013; Lüke and Frenzel, 2011).

and MAT), one linear trend variable, and one PCNM variable were selected as explanatory variables. All these selected variables explained 36.9% of the variation in the methanotroph communities. The environmental, linear trend, and PCNM variables explained 30.3%, 5.6%, and 6.1% of the variation, respectively. Moreover, spatial factors including both the linear trend and PCNM variables contributed 8.0% of the variation in methanotroph communities. All variation partitioning of environmental, linear trend, and PCNM variables were significant in an ANOVA test ($p < 0.05$). Therefore, both environmental factors and spatial distance were important factors to shape the structure of methanotroph communities. The environmental, linear trend, and PCNM variables purely explained 28.9%, 1.1%, and 1.9% of the variation, respectively. In total, spatial factors purely explained 6.6% of the variation in methanotroph communities. Therefore, compared with spatial distance, environmental properties were more important factors affecting the structure of methanotroph communities. We also performed variation partitioning using the 30 soil samples which we collected from the Tibetan Plateau (Fig. S1). In the forward selection process, three environmental variables (SWC, DTN, and NPS), one linear trend variable, as well as one PCNM variable were selected as explanatory variables. The results also showed that both environmental factors and spatial distance were significant factors, but environmental parameters were more important in shaping the structure of methanotroph communities.

4. Discussion

This study showed that the methanotroph communities in the upland grassland soils on the Qinghai-Tibetan Plateau were mainly dominated by USCγ, while JR3 were also abundant in some soils. Combined

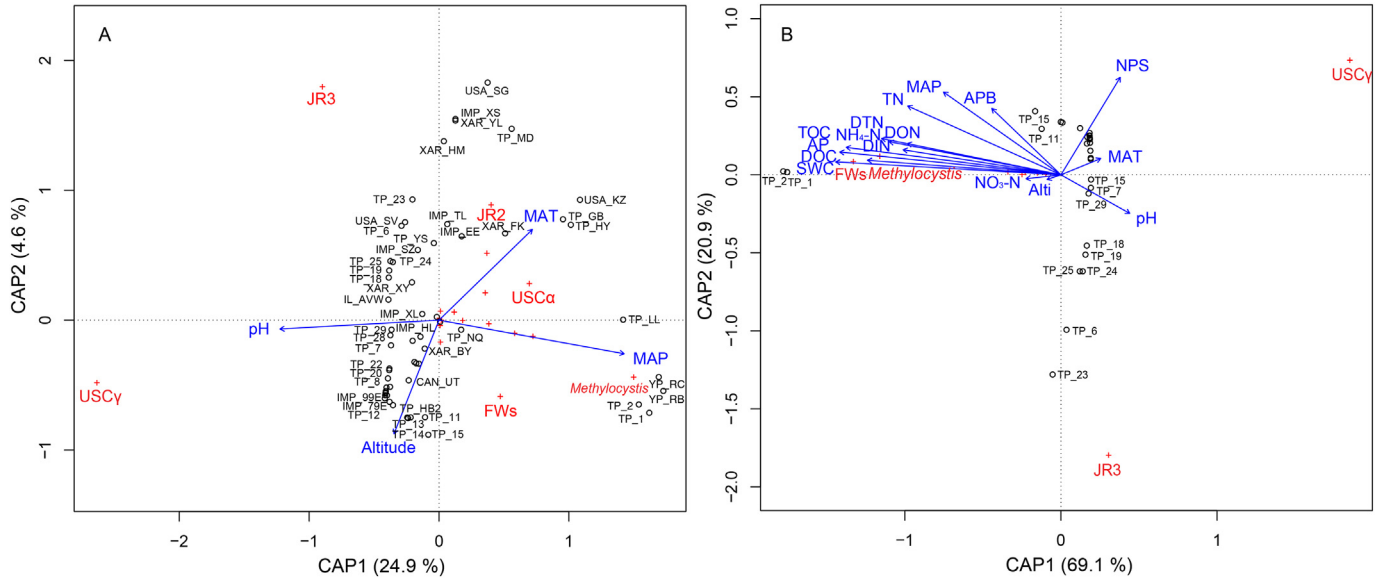

Fig. 4. The effect of environmental factors on methanotroph community composition was determined by Canonical Analysis of Principal Coordinates (CAP). (A) CAP for all the 63 grassland soil samples around the world. (B) CAP for the 30 soil samples collected on the Qinghai-Tibetan Plateau. Numbers next to symbols identify different sample sites. OTUs are shown as red plus signs (+) and are labeled with their cluster affiliations, including USCα, JR3, JR3, USCγ, *Methylocystis*, and FWs. (For interpretation of the references to colour in this figure legend, the reader is referred to the web version of this article.)

with soil samples in low MAP (<500 mm) grasslands around the world, USCγ and JR3 were almost the exclusive (>90%) *pmoA* clusters in 47 samples out of 55 samples. Both USCγ and JR3 are as yet uncultivated methanotrophic clusters. USCγ was discovered by Knief et al. (2003) and is believed to be responsible for atmospheric methane consumption (Knief, 2015); a draft genome sequence has been published (Edwards et al., 2017). USCγ and JR3 occur preferentially in upland soils and are affiliated with type Ic methanotrophs (Horz et al., 2005; Lüke and Frenzel, 2011). They have also been affiliated with the type Id group and referred to as USCγ sensu lato in a recent review (Knief, 2015). In previous studies, USCα, USCγ, and Jasper Ridge Clusters (JR1, JR2 and JR3) have been described as dominant methanotrophic clusters consuming methane at atmospheric concentration in upland soils (Horz et al., 2005; Knief et al., 2003; Holmes et al., 1999; Henckel et al., 2000; Knief et al., 2015); however, an extreme dominance of USCγ methanotrophs in upland grassland soils over a large spatial area, such as most grasslands on the Qinghai-Tibetan Plateau, even around the world, is to the best of our knowledge without precedence. Meanwhile, the *pmoA* sequences of USCα and JR1 are related to sequences of *Methylocapsa*, which belongs to type IIb methanotrophs within the Alphaproteobacteria; however, USCγ as well as JR2 and JR3 are related to type Ic methanotrophs within the Gammaproteobacteria (Lüke and Frenzel, 2011). Generally, Type I and Type II methanotrophs exhibit differences in the carbon fixation pathways, in the dominant phospholipid fatty acids and in other physiological traits. The metabolic activity of USCγ and JR2 methanotrophs should therefore be different to that of USCα methanotrophs. Thus, the upland grassland soils dominated by USCγ and JR2 methanotrophs might have different methane oxidation capacities compared with soils dominated by USCα methanotrophs. USCγ methanotrophs have only occasionally been reported to be relatively abundant among soil methanotrophs, e.g., in Chinese alpine meadow soils (Zheng et al., 2012), Israeli arid desert soils (Angel and Conrad, 2009) and Canadian upland tundra soils (Martineau et al., 2014); however, further investigations are needed to test whether USCγ also dominates the methanotroph communities in other upland soils. Meanwhile, it is still unproven that USCγ is able to maintain growth using atmospheric methane as their sole substrate. USCγ may require alternative carbon compounds, or maybe facultative as suggested for USCα methanotrophs (Pratscher et al., 2011; Pratscher et al., 2018). Successful isolation, or isotope probing, is needed to demonstrate the ability of USCγ to oxidize methane at ambient mixing ratios.

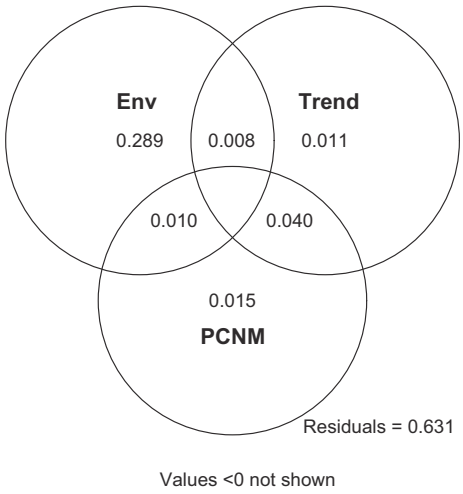

Fig. 6. Considering all the 63 samples, variation partitioning of methanotroph community structure by environmental variables (Env, top left) and the spatial factors including linear trend (Trend, top right) and principal coordinates of neighbor matrices variables (PCNM, bottom). A forward selection was used to select the best environmental, trend and PCNM variables for variation partitioning of methanotroph community structure.

Both USCα and USCγ methanotrophs are assumed to be involved in the oxidation of atmospheric methane in upland soils (Knief et al., 2003; Kolb, 2009). USCα methanotrophs were dominant in Tibetan grassland samples TP_HY and TP_GB with acidic soils (pH 5.8 and 6.0, respectively; Kou et al., 2017). Meanwhile, USCα methanotrophs were reported to be dominant in a variety of acidic to neutral upland forest soils (Jaatinen et al., 2004; Bengtson et al., 2009; Lima et al., 2014; Malghani et al., 2016). Most forest soils have pH values of 3.0–7.0, and generally forest soils are more acidic than grassland soils due to the continuous production of organic acids and CO_2 from decomposing litter (Osman, 2013). The acidic soils in forests provide suitable pH conditions for USCα methanotrophs. In contrast, USCγ has always been detected in neutral to alkaline soils (Knief et al., 2003; Kolb, 2009). The average pH

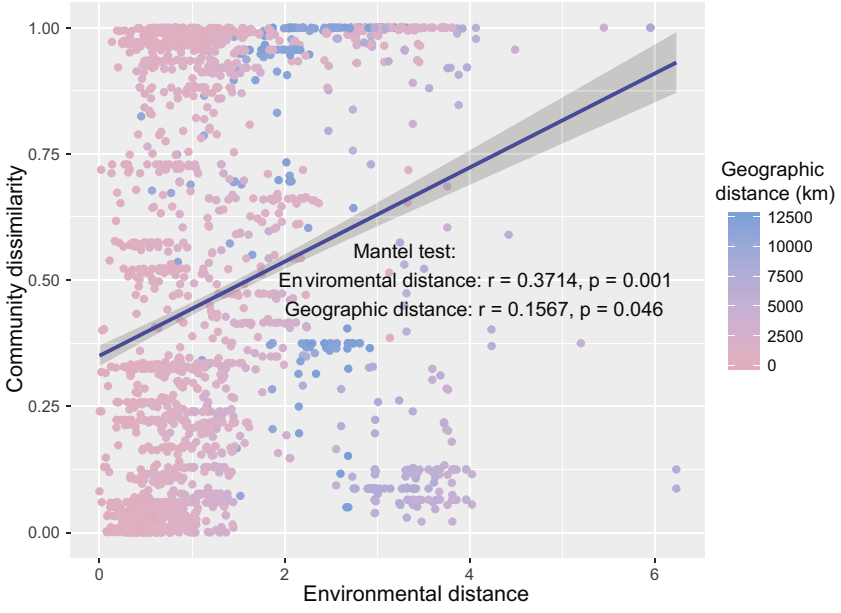

Fig. 5. Correlation between methanotroph community dissimilarities (Bray-Curtis distance) and environmental distances. Geographic distance was fitted on the methanotroph community dissimilarity. A fitted regression line on the graph illustrates the relationship between methanotroph community dissimilarity and environmental distance. The shaded area around the line is 0.95 confidence level. The relationships between methanotroph community and environmental or geographic distance were evaluated by Mantel tests.

values of soil samples with USCγ as the dominant methanotrophic cluster was 8.1. This might be one reason for the dominance of USCγ rather than USCα methanotrophs in the grassland soils included in this investigation. In addition, the discrimination of A189f/mb661r primer set against USCα methanotrophs was probably not the reason USCα were not detected in the 30 soil samples on the Qinghai-Tibetan plateau, since it was still not abundant when applying the two-round PCR approach.

Soil pH was an important factor that shaped methanotroph community structures in different forest soils (Kolb, 2009). USCγ was more likely to be detected in soils with pH > 6.0 than in acidic soils (Knief et al., 2003). In the CAP analyses including all 63 samples, pH was a significant environmental factor influencing the soil methanotroph community composition, and USCγ and was more abundant in soils with relatively high pH values; however, if only the 30 soils on the Qinghai-Tibetan Plateau were considered, no significant effect of soil pH on methanotroph community was observed which could be attributed to the narrow pH range (6.8–9.2) of the 30 soils. Furthermore, the high abundance of USCγ methanotrophs detected in these neutral and alkaline soils is consistent with previous reports that USCγ is associated with neutral and alkaline soils (Knief et al., 2003).

As revealed by the CAP analysis, MAP and SWC showed the strongest correlations with the methanotroph community profiles when considering all the 63 soil samples or only our 30 soil samples, respectively. This means that water availability is the most important factor affecting the distribution pattern of methanotroph communities in grassland soils. Soil moisture was reported to be positively correlated with USCα-like methanotroph diversity of grassland soils in Germany (Shrestha et al., 2012). This is in agreement with our results that soil methanotroph communities were different between soils in high and low MAP regions. Lower affinity methanotrophs such as *Methylocystis* and *Methylobacter* rather than USCγ and JR3 dominated soil methanotroph communities in high MAP and water content samples. High MAP and water content make soils more anaerobic, and thereby providing favorable ecological niche for anaerobic methanogenesis. Consequently, it increases the concentration of methane in soils, and thus the low affinity methanotrophs (e.g. *Methylocystis*) can survive and proliferate. Compared with grassland soils, the higher methane levels in wetland soils might be the reason why low affinity methanotrophs rather than USCγ and JR3 methanotrophs are there. Additionally, compared with upland grassland soils, the water content in wetland soils was relatively higher. The differences between soil methanotroph communities in wetland soils (Deng et al., 2013; Deng et al., 2016; Yun et al., 2010; Yun et al., 2014) and upland soils further highlights the important role of water availability for the distribution of methanotroph populations.

In this study, environmental factors were found to be more important than geographical distance in shaping the composition of methanotroph communities. The dominant methanotrophs in upland grassland soils were probably abundant since they were best adapted to the local environmental condition. In addition to MAP, SWC, and pH (as discussed above), soil nutrient content was negatively correlated with the relative abundance of USCγ and JR3 methanotrophs (see CAP analysis). This indicates that USCγ and JR3 methanotrophs have traits that allow them to outcompete other methanotrophs in relatively poor-nutrient soils. However, we should keep in mind that it was the total abundance of methanotrophs that was positively correlated with soil nutrient content, while the relative abundance of USCγ and JR3 methanotrophs was reduced. Further studies are necessary to allow prediction of methanotroph community composition from environmental habitat characteristics.

In conclusion, this study has shown that a high dominance of atmospheric methane oxidizers USCγ sensu lato methanotrophs in the examined upland grassland soils on the Qinghai-Tibetan Plateau and other upland grassland soils around the world. This study also provides strong evidence that environmental properties, such as MAP and soil pH, are more important than spatial distance in influencing the composition of the methanotroph populations.

Supplementary data to this article can be found online at https://doi.org/10.1016/j.scitotenv.2019.03.299.

Acknowledgements

We thank Desheng Wang for his assistance with Fig. 1. Support was obtained from Strategic Priority Research Program (B) of the Chinese Academy of Sciences (XDB15010201) and the Strategic Priority Research Program (A) of the Chinese Academy of Sciences (XDA20050103). We acknowledge further support by the National Natural Science Foundation of China (grant No. 31570518 and No. 41401075), National Key Research and Development Program of China (2016YFC0501800), Jiangsu Center for Collaborative Innovation in Geographical Information Resource Development and PAPD (No. 164320H116), Natural Science Foundation of Jiangsu Province, China (grant No. BK20181386).

Compliance with ethical standards

Conflict of interest

The authors declare that they have no conflict of interest.

References

Anderson, M.J., Willis, T.J., 2003. Canonical analysis of principal coordinates: a useful method of constrained ordination for ecology. Ecology 84, 511–525.
Angel, R., Conrad, R., 2009. In situ measurement of methane fluxes and analysis of transcribed particulate methane monooxygenase in desert soils. Environ. Microbiol. 11, 2598–2610.
Baani, M., Liesack, W., 2008. Two isozymes of particulate methane monooxygenase with different methane oxidation kinetics are found in *Methylocystis* sp strain SCZ. Proc. Natl. Acad. Sci. U. S. A. 105, 10203–10208.
Bengtson, P., Basiliko, N., Dumont, M.G., Hills, M., Murrell, J.C., Roy, R., Grayston, S.J., 2009. Links between methanotroph community composition and CH_4 oxidation in a pine forest soil. FEMS Microbiol. Ecol. 70, 356–366.
Bourne, D.G., McDonald, I.R., Murrell, J.C., 2001. Comparison of *pmoA* PCR primer sets as tools for investigating methanotroph diversity in three Danish soils. Appl. Environ. Microbiol. 67, 3802–3809.
Bray, J.R., Curtis, J.T., 1957. An ordination of the upland forest communities of southern Wisconsin. Ecol. Monogr. 27, 325–349.
Che, R., Deng, Y., Wang, F., Wang, W., Xu, Z., Hao, Y., Xue, K., Zhang, B., Tang, L., Zhou, H., et al., 2018. Autotrophic and symbiotic diazotrophs dominate nitrogen-fixing communities in Tibetan grassland soils. Sci. Total Environ. 639, 997–1006.
Conrad, R., 2007. Microbial ecology of methanogens and methanotrophs. Adv. Agron. 96, 1–63.
Conrad, R., 2009. The global methane cycle: recent advances in understanding the microbial processes involved. Environ. Microbiol. Rep. 1, 285–292.
Costello, A.M., Lidstrom, M.E., 1999. Molecular characterization of functional and phylogenetic genes from natural populations of methanotrophs in lake sediments. Appl. Environ. Microbiol. 65, 5066–5074.
Dai, Y., Wu, Z., Xie, S., Liu, Y., 2015. Methanotrophic community abundance and composition in plateau soils with different plant species and plantation ways. Appl. Microbiol. Biotechnol. 99, 9237–9244.
Deng, Y.C., Cui, X.Y., Lüke, C., Dumont, M.G., 2013. Aerobic methanotroph diversity in Riganqiao peatlands on the Qinghai-Tibetan Plateau. Environ. Microbiol. Rep. 5, 566–574.
Deng, Y., Cui, X., Dumont, M.G., 2016. Identification of active aerobic methanotrophs in plateau wetlands using DNA stable isotope probing. FEMS Microbiol. Lett. 363, fnw168.
Deza, M.M., Deza, E., 2009. Encyclopedia of distances. Encyclopedia of Distances. Springer, pp. 1–583.
Dray, S., Legendre, P., Blanchet, G., 2011. Packfor: Forward Selection with Permutation (Canoco p.46) (R package version 0.0–8/r100).
Dumont, M.G., Lüke, C., Deng, Y., Frenzel, P., 2014. Classification of *pmoA* amplicon pyrosequences using BLAST and the lowest common ancestor method in MEGAN. Front. Microbiol. 5, 34.
Dunfield, P.F., H.C. Reay, D.S., 2007. The soil methane sink. In: Smith, K.A., Grace, J. (Eds.), Greenhouse Gas Sinks. CAB International, Wallingford, UK, pp. 152–170.
Edgar, R.C., 2010. Search and clustering orders of magnitude faster than BLAST. Bioinformatics 26, 2460–2461.
Edgar, R.C., 2013. UPARSE: highly accurate OTU sequences from microbial amplicon reads. Nat. Methods 10, 996–998.
Editorial Board of Vegetation Map of China, 2001. Chinese Academy of Sciences. Vegetation Atlas of China (1:1000000) [M]. Science Press, Beijing, pp. 129–132.
Edwards, C.R., Onstott, T.C., Miller, J.M., Wiggins, J.B., Wang, W., Lee, C.K., Cary, S.C., Pointing, S.B., Lau, M.C.Y., 2017. Draft genome sequence of uncultured upland soil cluster *Gammaproteobacteria* gives molecular insights into high-affinity methanotrophy. Genome Announc. 5, e00047-17.
Henckel, T., Jackel, U., Schnell, S., Conrad, R., 2000. Molecular analyses of novel methanotrophic communities in forest soil that oxidize atmospheric methane. Appl. Environ. Microbiol. 66, 1801–1808.

Holmes, A.J., Costello, A., Lidstrom, M.E., Murrell, J.C., 1995. Evidence that particulate methane monooxygenase and ammonia monooxygenase may be evolutionarily related. FEMS Microbiol. Lett. 132, 203–208.
Holmes, A.J., Roslev, P., McDonald, I.R., Iversen, N., Henriksen, K., Murrell, J.C., 1999. Characterization of methanotrophic bacterial populations in soils showing atmospheric methane uptake. Appl. Environ. Microbiol. 65, 3312–3318.
Horz, H.P., Rich, V., Avrahami, S., Bohannan, B.J.M., 2005. Methane-oxidizing bacteria in a California upland grassland soil: diversity and response to simulated global change. Appl. Environ. Microbiol. 71, 2642–2652.
IPCC, 2014. Climate change 2014: synthesis report. Contribution of working groups I, II and III to the fifth assessment report of the intergovernmental panel on climate change. In: Core writing team, Pachauri, RK, Meyer, LA (Eds.), IPCC, Geneva, p. 151.
Jaatinen, K., Knief, C., Dunfield, P.F., Yrjala, K., Fritze, H., 2004. Methanotrophic bacteria in boreal forest soil after fire. FEMS Microbiol. Ecol. 50, 195–202.
Judd, C.R., Koyama, A., Simmons, M.P., Brewer, P., von Fischer, J.C., 2016. Co-variation in methanotroph community composition and activity in three temperate grassland soils. Soil Biol. Biochem. 95, 78–86.
Knief, C., 2015. Diversity and habitat preferences of cultivated and uncultivated aerobic methanotrophic bacteria evaluated based on *pmoA* as molecular marker. Front. Microbiol. 6, 1346.
Knief, C., Lipski, A., Dunfield, P.F., 2003. Diversity and activity of methanotrophic bacteria in different upland soils. Appl. Environ. Microbiol. 69, 6703–6714.
Kolb, S., 2009. The quest for atmospheric methane oxidizers in forest soils. Environ. Microbiol. Rep. 1, 336–346.
Kolb, S., Knief, C., Stubner, S., Conrad, R., 2003. Quantitative detection of methanotrophs in soil by novel *pmoA*-targeted real-time PCR assays. Appl. Environ. Microbiol. 69, 2423–2429.
Kou, Y., Li, J., Wang, Y., Li, C., Tu, B., Yao, M., Li, X., 2017. Scale-dependent key drivers controlling methane oxidation potential in Chinese grassland soils. Soil Biol. Biochem. 111, 104–114.
Legendre, P., Fortin, M.J., 2010. Comparison of the mantel test and alternative approaches for detecting complex multivariate relationships in the spatial analysis of genetic data. Mol. Ecol. Resour. 10, 831–844.
Legendre, P., Legendre, L., 2012. Numerical Ecology. Elsevier Science, Amsterdam, the Netherlands.
Lima, A.B., Muniz, A.W., Dumont, M.G., 2014. Activity and abundance of methane-oxidizing bacteria in secondary forest and manioc plantations of Amazonian Dark Earth and their adjacent soils. Front. Microbiol. 5, 550.
Ludwig, W., Strunk, O., Westram, R., Richter, L., Meier, H., Yadhukumar, Buchner, A., Lai, T., Steppi, S., Jobb, G., et al., 2004. ARB: a software environment for sequence data. Nucleic Acids Res. 32, 1363–1371.
Lüke, C., Frenzel, P., 2011. Potential of *pmoA* amplicon pyrosequencing for methanotroph diversity studies. Appl. Environ. Microbiol. 77, 6305–6309.
Ma, T., Chen, H., Wang, Y., Kang, X., Tian, J., Zhou, X., Zhu, Q., Peng, C., Liu, L., Hu, J., et al., 2016. Effects of enclosure time on the community composition of methanotrophs in the soils of the Inner Mongolia grasslands. J. Soils Sediments 16, 1022–1031.
Malghani, S., Reim, A., von Fischer, J., Conrad, R., Kuebler, K., Trumbore, S.E., 2016. Soil methanotroph abundance and community composition are not influenced by substrate availability in laboratory incubations. Soil Biol. Biochem. 101, 184–194.
Martineau, C., Pan, Y., Bodrossy, L., Yergeau, E., Whyte, L.G., Greer, C.W., 2014. Atmospheric methane oxidizers are present and active in Canadian high Arctic soils. FEMS Microbiol. Ecol. 89, 257–269.
Oksanen, J., Blanchet, F.G., Kindt, R., Legendre, P., Minchin, P.R., O'Hara, R.B., Simpson, G.L., Solymos, P., Stevens, M.H.H., Wagner, H., 2014. Vegan Community Ecology Package (R Package Version 2.2-0).
Olsen, S.R., 1954. Estimation of Available Phosphorus in Soils by Extraction with SodiumBicarbonate. United States Department Of Agriculture, Washington.
Osman, K.T., 2013. Forest Soils: Properties and Management. Springer Science & Business Media.
Pratscher, J., Dumont, M.G., Conrad, R., 2011. Assimilation of acetate by the putative atmospheric methane oxidizers belonging to the USC alpha clade. Environ. Microbiol. 13, 2692–2701.
Pratscher, J., Vollmers, J., Wiegand, S., Dumont, M.G., Kaster, A.-K., 2018. Unravelling the identity, metabolic potential, and global biogeography of the atmospheric methane-oxidising upland soil cluster α. Environ. Microbiol. 20, 1016–1029.
Schloss, P.D., Westcott, S.L., Ryabin, T., Hall, J.R., Hartmann, M., Hollister, E.B., Lesniewski, R.A., Oakley, B.B., Parks, D.H., Robinson, C.J., 2009. Introducing mothur: open-source, platform-independent, community-supported software for describing and comparing microbial communities. Appl. Environ. Microbiol. 75, 7537–7541.
Semrau, J.D., Dispirito, A.A., Yoon, S., 2010. Methanotrophs and copper. FEMS Microbiol. Rev. 34, 496–531.
Shrestha, P.M., Kammann, C., Lenhart, K., Dam, B., Liesack, W., 2012. Linking activity, composition and seasonal dynamics of atmospheric methane oxidizers in a meadow soil. ISME J. 6, 1115–1126.
Vincenty, T., 1975. Direct and inverse solutions of geodesics on the ellipsoid with application of nested equations. Surv. Rev. 23, 88–93.
Wei, D., Xu, R., Tenzin, T., Wang, Y.S., Wang, Y.H., 2015. Considerable methane uptake by alpine grasslands despite the cold climate: in situ measurements on the central Tibetan Plateau, 2008-2013. Glob. Chang. Biol. 21, 777–788.
Wickham, H., 2009. ggplot2: Elegant Graphics for Data Analysis. Springer Science & Business Media.
Wuebbles, D.J., Hayhoe, K., 2002. Atmospheric methane and global change. Earth-Sci. Rev. 57, 177–210.
Yimga, M.T., Dunfield, P.F., Ricke, P., Heyer, H., Liesack, W., 2003. Wide distribution of a novel *pmoA*-like gene copy among type II methanotrophs, and its expression in *Methylocystis* strain SC2. Appl. Environ. Microbiol. 69, 5593–5602.
Yun, J.L., Ma, A.Z., Li, Y.M., Zhuang, G.Q., Wang, Y.F., Zhang, H.X., 2010. Diversity of methanotrophs in Zoige wetland soils under both anaerobic and aerobic conditions. J. Environ. Sci. (China) 22, 1232–1238.
Yun, J.L., Ju, Y.W., Deng, Y.C., Zhang, H.X., 2014. Bacterial community structure in two permafrost wetlands on the Tibetan Plateau and Sanjiang Plain, China. Microb. Ecol. 68, 360–369.
Zheng, Y., Yang, W., Sun, X., Wang, S.P., Rui, Y.C., Luo, C.Y., Guo, L.D., 2012. Methanotrophic community structure and activity under warming and grazing of alpine meadow on the Tibetan Plateau. Appl. Microbiol. Biotechnol. 93, 2193–2203.